Astron. Astrophys. 279, 298–309 (1993)

ASTRONOMY AND ASTROPHYSICS

Atomic data from the IRON Project

I. Goals and methods

D.G. Hummer[1,2], K.A. Berrington[3], W. Eissner[3], Anil K. Pradhan[4], H.E. Saraph[5], and J.A. Tully[6]

[1] Max-Planck-Institut für Astrophysik, Karl-Schwarzschild-Str. 1, D-85748 Garching bei München, Germany
[2] Institut für Astronomie und Astrophysik der Universität München, Scheinerstr. 1, D-81679 München 80, Germany
[3] Department of Applied Mathematics and Theoretical Physics, The Queen's University, Belfast BT7 1NN, UK
[4] Department of Astronomy, The Ohio State University, Columbus, Ohio 43210-1106, USA
[5] Department of Physics and Astronomy, University College London, Gower Street, London WC1E 6BT, UK
[6] Observatoire de la Côte d'Azur, URA 1362 du C.N.R.S., B.P. 229, 06304 Nice Cedex 4, France

Received May 18, accepted June 7, 1993

Abstract. The IRON Project has the goal of computing on a large scale electron excitation cross sections and rates of astrophysical and technological importance, using the most reliable procedures currently available. Radiative transition probabilities and photoionization cross sections not known from other sources e. g. from the Opacity Project, will also be presented. Although the major effort will be for ions of the iron-group elements, other ions of astrophysical interest will also be included. In this introductory paper models and procedures to be used are summarized and the approximations are discussed. As an example of our computational procedures, typical results for fine structure transitions involving electron collisions with Fe XVIII ions and radiative data from Fe XVII are presented.

Key words: atomic data – electron collision rates – fine structure transitions

1. Introduction

The paucity of reliable electron excitation cross sections or rate coefficients has long hindered the quanitative analysis of astronomical spectra. Information concerning the physical state of the gas in objects for which LTE is not valid can be extracted from spectra only to the extent that collisional rates coupling the electrons to the radiating atoms and ions are known.

The primary goal of the IRON Project is to systematically compute reliable ab-initio electron excitation cross sections for astrophysical applications. These data will complement the very extensive radiative data computed in the Opacity Project (cf. Seaton et al. 1993) which is now available with the data server TOPBASE (Cunto & Mendoza 1992). Particular attention is given to cross sections required for the interpretation of data from specific space observations. Radiative transition probabilities not already calculated by the Opacity Project will also be provided, especially those for electric quadrupole and magnetic dipole transitions as well as for electric dipole cases in which fine structure must be taken into account.

Because of the complexity of the Project, in particular its computational aspects, short-term and long-term goals have been identified and are being actively pursued by an international collaboration.

The first stage of the Project concerns the excitation rate coefficients for fine structure transitions in the ground configuration of astrophysically important ions in the iso-electronic sequences B, C, O, F, Al, Si, S, and Cl. These data are essential for the interpretation of infra-red lines to be observed by the Infrared Space Observatory (ISO), as well as for coronal spectra. The calculations of fine structure and all other transitions in the ground configuration of the relevant ions are substantially completed and will be published shortly in a series of papers in A&A, to which this paper provides an introduction.

The second stage of the Project, which concentrates on the ions of iron, is now under way. Cross sections are now being calculated for all transitions in all ions of iron between states with principal quantum number up to at least $n = 3$ and when possible, to $n = 4$. This will provide collisional rates for interpretation of observations from the Solar and Heliospheric Observatory (SOHO). In particular, reliable collisional and radiative data will become available for Fe II, which appears in the spectra of an enormous variety of objects (cf. Viotti et al. 1988).

In general, as the capability for UV and XUV observations grows, reliable iron-ion collisional rates will become essential, as the spectra of many objects are dominated by iron lines. For example, the lines of Fe II through Fe VII are very prominent in the UV spectra of O-type stars, which can be observed to great

Send offprint requests to: D.G. Hummer

distances. Precise iron-group abundances can be obtained for many other galaxies by non-LTE spectrum synthesis once the IRON Project data becomes available.

The IRON Project is based on the use of the R-matrix method for the solution of the many-body Schrödinger equation for both radiative and collisional processes. It is appropriate to discuss this method in the hierarchy of models used for calculating collisional data. At high energies, and particularly for highly charged ions, perturbative methods such as the distorted wave (D.W.) and Coulomb-Born approximation can be efficient and reasonably accurate; for a systematic discussion of these approximations, see the review by Henry (1993). But at lower energies, a proper treatment must allow for the many-body Coulomb nature of the problem by a full quantum mechanical description in which all electrons are treated equivalently, at least in a local region. Ab initio calculations therefore usually employ a configuration-interaction treatment, in which all target states strongly coupled to the initial and final states of interest are included in the expansion of the total collision wavefunction. The R-matrix method can be considered to be a computationally efficient way of solving the resulting"close-coupling" equations (Burke & Eissner 1983).

For some of the ions to be treated in the IRON Project, data are already available in the literature from previous close-coupling or R-matrix calculations. These data will be evaluated during the course of the Project, and if necessary recalculated with higher accuracy using the new developments of the Project, by using, for example, more accurate target wave functions, coupling to higher states, a more consistent treatment of relativistic effects, etc. A systematic approach will be used to obtain data of comparable accuracy throughout iso-electronic sequences, which has rarely been done before.

Without additional modification, the close-coupling or R-matrix approach can be used reliably only for scattering energies below the ionization threshold. To overcome this limitation, the Intermediate Energy R-matrix Method (Burke et al. 1987) is under development and is now being used for hydrogenic systems (cf. Scholz et al. 1990). This method will be employed when necessary to widen the scope of the Project.

The IRON Project aims to obtain highly accurate atomic data, by systematic refinements of the theoretical models and numerical approximations used, and by comparisons with experimental data where possible.

In Sect. 2 the theoretical and computational methods used in this work are outlined. The calculation of radiative rates and photoionization cross sections including electric dipole and magnetic dipole transitions is discussed in Sect. 3. In Sect. 4 the calculation of collision rates from the cross sections and the presentation of collision rate coefficients is summarized. To illustrate the various levels of approximation at which these calculations can be made, the results for Fe XVIII are discussed in detail in Sect. 5. In the concluding section the status of work underway is reported.

2. Collision theory

An *ab initio* treatment is employed for the collision of an electron with an isolated atom or ion. Consider the time independent Schrödinger equation

$$H_{N+1}\Psi = E\Psi. \tag{1}$$

The total wavefunction Ψ of the system with total energy E is calculated numerically using R-matrix techniques.

For processing on a computer, pure number equations are needed, preferably on a scale in which all quantities are of order one. As an energy unit it is natural to choose the hydrogenic ionization energy of 1 Ry = $(\alpha^2/2)\cdot m_0c^2$ =13.6058... eV, related to the electron rest mass by the electromagnetic coupling parameter or 'fine structure constant' α = 1/137.036. Then the non-relativistic Hamiltonian for N target electrons plus a scattering electron in the field of an atomic nucleus with electric charge number Z reads

$$H_{N+1} = \sum_{i=1}^{N+1}\left\{-\nabla_i^2 - \frac{2Z}{r_i} + \sum_{j>i}^{N+1}\frac{2}{r_{ij}}\right\}. \tag{2}$$

Here radial distances are given in units of the Bohr radius $a_0 = \hbar/(\alpha m_0 c) = 0.52918\ldots\times 10^{-8}$ cm. Also, $r_{ij} = |\boldsymbol{r}_i - \boldsymbol{r}_j|$, where $\boldsymbol{r}_i$ is the radius vector of electron i with respect to the target nucleus, which is assumed to have infinite mass. Wave numbers k are then given in units of $1/a_0$ and the unit of time is $\tau_0 = 2a_0/(\alpha c) = 4.838\cdot 10^{-17}$s.

With the Hamiltonian (2) the Schrödinger equation (1) can be solved in Russell-Saunders (LS) coupling, which is adequate for electron scattering on light atoms, where both Z and the residual charge $z = Z - N$ are small. Orbital L and spin S angular momenta and parity π are conserved separately. Thus an SL term is labelled by $^{2S+1}L^{\pi}$.

The IRON Project also involves heavy atoms, but not much beyond Z = 30. Therefore they are treated in the low-Z Breit-Pauli (BP) approximation (or more simply, by recoupling LS results as in Subsect. 2.6. Here the Hamiltonian in the BP approximation is taken as

$$H_{N+1}^{\rm BP} = H_{N+1} + H_{N+1}^{\rm mass} + H_{N+1}^{\rm Dar} + H_{N+1}^{\rm so}, \tag{3}$$

where H_{N+1} is the non-relativistic Hamiltonian defined by Eq. (2), together with the one-body mass correction term, the Darwin term and the spin-orbit term resulting from the reduction of the Dirac equation to Pauli form. The mass-correction and Darwin terms do not break the LS symmetry, and they can therefore be retained with great effect in computationally cheaper LS calculations. Spin-orbit interaction does, however, split the LS *terms* into *fine structure levels* labelled by J^{π}, where J=L+S is the total angular momentum.

Although the BP approach has been used for atoms as heavy as mercury, a more satisfactory approach for such heavy targets is to use the Dirac Hamiltonian. This has been developed as a practical approach for calculating electron-atom and electron-ion scattering by Norrington & Grant (1981, 1987). Although

such an elaborate treatment should not be necessary for IRON Project ions, one or two ions of Fe will nevertheless be treated with the Dirac R-matrix method in order to check the validity of the BP approximation that is used.

2.1. The target description

In order to carry out a collision calculation involving an atom or ion, the N-electron target states must first be defined. The target is described using *ab initio* atomic structure techniques.

Define a set of target eigenstates, and possibly pseudostates, Φ_i and their corresponding eigenenergies ϵ_i by the equation

$$\langle \Phi_i \mid H_N \mid \Phi_j \rangle = \epsilon_i \delta_{ij}, \tag{4}$$

where H_N is the target Hamiltonian defined by Eq. (2) with N+1 replaced by N. The pseudostates are constructed to allow, to some extent, for the infinity of states necessarily omitted. These eigenstates are usually written as a configuration interaction (CI) expansion in terms of some basis configurations ϕ_i by

$$\Phi_i(\mathbf{x}_1 \ldots \mathbf{x}_N) = \sum_j \phi_j(\mathbf{x}_1 \ldots \mathbf{x}_N) c_{ji}, \tag{5}$$

where $x_i \equiv \boldsymbol{r}_i \sigma_i = \hat{\mathbf{r}}_i r_i, \sigma_i$ represents the space and spin coordinates of the i th electron and the coefficients c_{ji} are determined by diagonalizing the target Hamiltonian in Eq. (4) (e. g. Eissner et al. 1974; Hibbert 1975). The target state or pseudostate in Eqs. (4) and (5) has total orbital and spin angular momenta L_i, S_i and parity π_i, or J_i and π_i in the relativistic case.

The ϕ_i are constructed from a bound orbital basis usually consisting of self consistent field (SCF) orbitals plus some additional pseudo-orbitals included to represent electron correlation effects. Current R-matrix computer programs require that the same orthonormal set of one-electron orbitals be used to describe all of the target states.

The accuracy of the resulting wavefunctions depends on both the truncation of the CI expansion (5) and the choice of radial orbitals, and can be checked by comparing the calculated target energies and oscillator strengths with experiment. It should be emphasized that a major, though largely unseen, workload of the IRON Project is the development of good target wavefunctions, particulary for excited states, to use in the collision calculations.

Two BP atomic multiconfigurational packages, CIV3 and SUPERSTRUCTURE, are used to develop suitable targets and to provide radial orbital functions for input to the R-matrix programs. They can also provide the target state energies and CI coefficients.

CIV3 (Hibbert 1975) uses Slater-type orbitals (STOs) to represent the CI functions, which are optimized by minimizing the target energies. Either a single energy level or a weighted sum of energies can be minimized. Normally Hartree-Fock orbitals as tabulated by Clementi & Roetti (1974) are taken to define the core electrons, and CIV3 provides excited-state orbitals, plus any extra correlation or pseudo-orbitals needed to improve the target wavefunctions. Polarized pseudostates can also be generated.

SUPERSTRUCTURE (Eissner et al. 1974; Eissner 1991) generates radial orbitals from numerical integrations of central-field equations. As the potential for computing spectroscopic orbitals one takes the solution $V(r/\lambda; Z, N)$ of a Thomas-Fermi-Dirac-Amaldi statistical model (SM) potential equation, with the scaling parameter λ_{nl} — normally close to 1.0 — determined variationally by optimizing a suitable functional, usually the energy sum over all the spectroscopic target terms of interest. Correlation orbitals can be computed in a SM potential with $\bar{\lambda} \gg 1$, though a much better correlation potential in terms of an effective charge, proposed by Nussbaumer & Storey (1978), is normally used. Further options in SUPERSTRUCTURE relevant to the current work are the inclusion of terms of BP order in radiative operators, especially for magnetic dipole transitions (Eissner & Zeippen 1981), and computation of magnetic quadrupole transitions M2.

2.2. The collision — internal region

R-matrix theory starts by partitioning configuration space into two regions by a sphere of radius a centred on the target nucleus (Burke et al. 1971).

In the internal region $r \leq a$, where r is the relative coordinate of the scattered electron and the target nucleus, electron exchange and correlation between the scattered electron and the N-electron target atom or ion are important and the (N+1)-electron collision complex is similar to a bound state. Consequently, a configuration interaction (CI) expansion of this complex, analogous to that used in bound state calculations, is adopted. In the external region, $r > a$, electron exchange between the scattered electron and the target can be neglected if the radius a is chosen so that the charge distribution of the target is contained within the sphere. The fact that exchange and correlation effects are confined to a small volume enables an R-matrix approach to be appropriate even in the presence of long-range Coulomb potentials.

In order to solve Eq. (1) in the internal region, introduce basis states ψ_i by the equation

$$\langle \psi_k | H_{N+1} | \psi_{k'} \rangle_{\rm int} = E_k \delta_{kk'}, \tag{6}$$

where the integration over the radial variables is restricted to the internal region. These basis states are expanded in the form

$$\psi_k(\mathbf{x}_1 \ldots \mathbf{x}_{N+1}) =$$

$$\mathcal{A} \sum_{ij} \overline{\Phi}_i(\mathbf{x}_1 \ldots \mathbf{x}_N; \hat{\mathbf{r}}_{N+1}\sigma_{N+1}) r_{N+1}^{-1} u_j(r_{N+1}) a_{ijk} + \sum_i \chi_i(\mathbf{x}_1 \ldots \mathbf{x}_{N+1}) b_{ik}, \tag{7}$$

where $\mathcal{A}$ is the antisymmetrization operator, which ensures that the total wave function is antisymmetric in accordance with the Pauli exclusion principle; the channel functions $\overline{\Phi}_i$ are obtained by coupling the target states Φ_i, defined by Eqs. (4) and (5), with the angular and spin functions of the scattered electron to

form eigenstates of the total orbital and spin angular momenta and parity; the quadratically integrable (L^2) functions χ_i, which vanish on the surface of the internal region, are formed from the bound orbital basis and are included to allow for electron correlation effects and to ensure completeness of the total wave function. The continuum orbital basis functions u_j, which represent the motion of the scattered electron, are non-zero on the surface of the internal region, and will be discussed further below. The coefficients a_{ijk} and b_{ik} in Eq. (7) are determined by diagonalizing the collisional Hamiltonian.

The total wavefunction Ψ in the internal region can be expanded in terms of these basis states ψ_k as

$$\Psi = \sum_k \psi_k A_{kE}, \tag{8}$$

where the A_{kE} are the expansion coefficients for a given total energy E. Projecting this equation onto the channel functions $\overline{\Phi}_i$ and evaluating on the boundary of the internal region yields the reduced radial wave functions:

$$F_i(a) = \sum_j R_{ij}(E) \cdot \left(a\frac{\mathrm{d}F_j}{\mathrm{d}r} - bF_j \right)_{r=a}, \tag{9}$$

which introduces the R-matrix, defined by

$$R_{ij}(E) = \frac{1}{a}\sum_k \frac{w_{ik}w_{jk}}{E_k - E} + R_i^{\mathrm{B}}(E)\delta_{ij}; \tag{10}$$

here $R_i^{\mathrm{B}}(E)$ is a 'Buttle' correction, discussed futher below. The eigenvalues E_k and the surface amplitudes w_{ik} are determined by diagonalizing the Hamiltonian matrix in Eq. (6) once for each set of conserved quantum numbers associated with the total angular momentum and parity of the electron-atom system. Eqs. (9) and (10) describe the solution of the electron atom (ion) scattering problem in the internal region, and must be matched to the external region solutions.

Note that Eq. (10) implies that the R-matrix is known for all energies once the w_{ik} and E_k have been obtained. Thus the R-matrix method is highly efficient when large numbers of scattering energies are required, for example, to elucidate complicated resonance structures in collision strengths, or to locate large numbers of bound states in radiative data applications.

Note also that as Eq. (7) has the form of a close coupling expansion including correlation terms, it contains all the important features of the low energy scattering process such as electron exchange, channel coupling, resonance effects, etc. However, at intermediate energies, a highly correlated wavefunction can give rise to unphysical pseudoresonances which must be averaged in an appropriate way to yield the required cross section (Burke et al. 1981).

A further point concerns target energy adjustments. It can be shown from Eqs. (2), (4) and (7) that the continuum-continuum part of the Hamiltonian matrix defined by Eq. (6) (ie. involving the first summation of Eq. (7)) may be split into the sum of two matrices, one of which is diagonal and contains the eigenenergies of the target atom. This allows the possibility of adjusting the diagonal elements of the internal region matrix before diagonalization to reproduce the observed energy spectrum of the target, and to correctly account for the kinematics of the continuum electron in the external region. In practice, accurate energies may not be available for all the target states included in the calculation; also it is difficult to make a consistent adjustment to the bound-bound part of Eq. (6) (ie. involving the second summation of Eq. (7)). Nevertheless, the incorporation of observed energies into the calculation can be advantageous (for an example, see Le Dourneuf et al. 1979), and will be considered during the IRON project.

Finally, consider the reduced radial continuum orbitals $u_j(r)$. The truncation of the continuum basis in Eqs. (7) and (10) is a further approximation in the R-matrix method. This approximation is independent of that arising from the truncation of the close coupling expansion itself, and can limit the energy range in which the method is valid. In principle, members of any complete set of functions satisfying appropriate boundary conditions at $r = 0$ and $r = a$ can be used. However, a careful choice will lead to more rapid convergence of the R-matrix.

Here the $u_j(r)$ are obtained by solving a model single-channel scattering problem for each angular momentum l, subject to homogeneous boundary conditions at $r = a$, following the work of Burke et al. (1971). This approach gives accurate results provided that a correction ($R_i^B(E)$ in Eq. (10)) proposed by Buttle (1967), to allow for the omitted high lying poles in the R-matrix expansion, is included. Since such corrections vary smoothly with energy, they can be fitted to an analytic function (Seaton 1987a) for computational economy. The continuum orbitals are normally Lagrange orthogonalized to bound orbitals $P_k(r)$ of the same angular symmetry, though Schmidt orthogonalization is usually adopted for pseudo-orbitals. The latter procedure usually gives better convergence, but numerical errors associated with overcompleteness of the basis can arise if the number of orbitals involved is large, for example when high impact energies are required.

2.3. The collision — external region

The next step is the solution of the electron-atom scattering problem when the scattered electron is in the external region $r > a$.

In this region electron exchange between the scattered electron and the target can be neglected if the radius a is chosen so that the charge distribution of the target is contained within the sphere. The scattered electron then moves in the long-range multipole potential of the target. This potential is local, and the solution in this region can be obtained using a standard method for solving coupled differential equations together with an asymptotic expansion or by using perturbation theory. By analogy with Eq. (7) the total wave function is expanded in this region in a close-coupling form

$$\Psi(\mathbf{x}_1 \ldots \mathbf{x}_{N+1}) = \sum_i \overline{\Phi}_i \ (\mathbf{x}_1 \ldots \mathbf{x}_N; \hat{\mathbf{r}}_{N+1}\sigma_{N+1}) r_{N+1}^{-1} F_i(r_{N+1}) \tag{11}$$

where the $\overline{\Phi}_i$ are the same set of channel functions used in Eq. (7), but now no antisymmetrisation between the scattered and target electrons is required since they occupy different regions of space. Substituting Eq. (11) into Eq. (1) and projecting onto the channel functions yields a set of coupled differential equations satisfied by the reduced radial wave functions $F_i(r)$ of the form

$$\left(\frac{\mathrm{d}^2}{\mathrm{d}r^2} - \frac{l_i(l_i+1)}{r^2} + \frac{2Z}{r} + k_i^2\right) F_i(r) = 2\sum_{j=1}^{n} V_{ij}(r)F_j(r), \quad i = 1 \ldots n,\ r \geq a \tag{12}$$

Here n is the number of channel functions retained in the expansion (7), l_i are the channel angular momenta, k_i^2 are the channel energies defined in terms of the target energies ϵ_i by

$$k_i^2 = E - \epsilon_i \tag{13}$$

and the potential matrix V_{ij} can be represented as an expansion in inverse powers of r. Often the channel coupling for electron-ion scattering is dominated by the first non-zero multipole in the potential, in which case the use of perturbed Coulomb functions can lead to highly efficient algorithms (Berrington et al. 1987) for solving Eqs. (12). The boundary conditions at infinity are

$$F_{ij}(r) \underset{r\to\infty}{\sim} \sqrt{k_i}\,(\sin\theta_i\,\delta_{ij} + \cos\theta_i\,K_{ij}), \quad \text{open channels} \quad (k_i^2 \geq 0), \tag{14}$$

$$F_{ij}(r) \underset{r\to\infty}{\sim} r^{\nu}\exp(-\frac{k}{\nu}r) \longrightarrow 0, \quad \text{closed channels} \quad (k_i^2 \equiv -z^2/\nu^2 < 0), \tag{15}$$

where the second index j on F_{ij} distinguishes the n_a linearly independent solutions of Eqs. (12), n_a is the number of open channels, and θ_i is the phase of the regular Coulomb function. Eqs. (12) are thus integrated outwards subject to the R-matrix boundary conditions Eq. (9) at $r = a$ and then fitted to an asymptotic expansion to determine the $n_a \times n_a$ reactance matrix (K).

There are a number of computer programs for solving the coupled Eqs. (12) in the external region. For the IRON Project, a new external-region module STGFJ has been written for positive ion targets, using a perturbation technique as in the Opacity Project module STGF (Berrington et al. 1987). STGFJ can produce K matrices in LS coupling or intermediate coupling, either by interfacing directly with the internal region BP R-matrix program or by transforming LS coupled K-matrices (Saraph 1972, 1978) (see subsections 2.5 and 2.6), including detailed resonance structure as well as resonance averages using the Gailitis formulation (cf. Seaton 1983). It can also produce the external region radial functions $F(r)$, required for bound-free and free-free radiative calculations.

Other external region programs can be used in place of STGFJ to solve the external region problem. In particular, FARM (Noble & Burke 1993), a new and highly optimized program incorporating the R-matrix propagator techniques of Baluja et al. (1982), Light & Walker (1976) and Light et al. (1979), together with the accelerated asymptotic expansion method of Noble & Nesbet (1984), for solving the coupled Eqs. (12) can be used for both neutral and ionic targets – though constrained at present to electron collisions in LS coupling.

It follows from the preceding discussions, that while the R-matrix is determined by a single diagonalization in the internal region for all energies, the coupled Eqs. (12) must be solved for $r \geq a$ to yield the solutions F_{ij} and hence the K-matrix, S-matrix and cross section for each energy of interest.

2.4. The collision strength and cross section

The K-matrix contains all the information needed to derive the observables associated with electron collisions. In particular, the $n_a \times n_a$ scattering matrix (S) is given by the matrix equation

$$\mathbf{S} = \frac{\mathbf{1} + \mathrm{i}\mathbf{K}}{\mathbf{1} - \mathrm{i}\mathbf{K}}\,. \tag{16}$$

S-matrix elements determine the collision strength for a transition from an initial target state i to a final target state f:

$$\Omega_{if} = \frac{1}{2}\sum w \mid S_{if} - \delta_{if} \mid^2, \tag{17}$$

where $w = (2L + 1)(2S + 1)$ or $(2J + 1)$ depending on the coupling scheme, and the summation runs over the partial waves and channels coupling the initial and final states of interest.

The total angular momentum (L or J) range in the summation of Eq. (17) is infinite. However, the collision strength is normally dominated by low angular momentum partial waves, at least at low collision energies. The exception concerns allowed transitions, where a "top-up" procedure, based on the Burgess sum rule, is employed to extrapolate the finite sum (Burke & Seaton 1986).

The collision strength determines the excitation cross section σ_{if} as a physical quantity:

$$\sigma_{if} = \Omega_{if}\frac{\pi a_0^2}{w_i k_i^2}, \tag{18}$$

w_i being the statistical weight of the initial target state $\left(w_i = (2S_i{+}1)(2L_i{+}1)\right.$ or $\left.2J_i{+}1\right.$, depending on the coupling scheme$\left.\right)$, and k_i^2 equals the incident electron energy in Rydbergs.

A general computer program RMATRX for calculating electron-atom and electron-ion cross sections, as well as atomic and ionic photoionization cross sections and polarizabilities, based on the non-relativistic Hamiltonian of Eq. (2) has been written by Berrington et al. (1974, 1978, 1987). This program has been widely used to calculate a large quantity of atomic data for low Z atoms and ions, normally in the LS coupling scheme. Further developments have been made to include relativistic effects in these programs, as described in the next two subsections.

2.5. Relativistic effects — the BP Hamiltonian

As the nuclear charge Z increases, relativistic effects in both the target wave function and the wave function representing

the scattered electron become important even for low energy electron scattering.

The conserved quantum numbers are now JM_J and π rather than LSM_LM_S and π, and thus the corresponding Hamiltonian matrix analogous to the non-relativistic Eq. (6) is much larger, increasing considerably the computational effort. An *intermediate coupling* representation is used in which j, the total angular momentum of the core, is coupled to l and s (the electron spin 1/2), the orbital angular momentum and spin of the added electron in the following way:

$$\mathbf{j} + \mathbf{l} = \mathbf{K}, \qquad \mathbf{K} + \mathbf{s} = \mathbf{J}, \tag{19}$$

where K is an intermediate quantum number.

The non-relativistic R-matrix method has been extended by Scott & Burke (1980) to include the BP Hamiltonian given by Eq. (3). Hamiltonian matrix elements calculated in LS coupling are augmented and transformed as described and programmed by Scott & Taylor (1982).

For the IRON Project, the Scott and Taylor BP package has been merged with the non-relativistic Opacity Project package, with switches in the input data controlling whether or not the various relativistic options are to be included. Some limitations of the original programs have been overcome, for example, in the evaluation of radiative data in intermediate coupling. Also the effective spin-orbit parameters ζ_{nl} can now be calculated, following Blume & Watson (1962), which alleviates the effects of omitted 2-body fine structure operators where it matters most – for closed shells.

2.6. Relativistic effects by recoupling

An alternative procedure for treating relativistic effects is based on a recoupling of the LS transition amplitudes to obtain collision strengths between fine structure levels, as in the program JAJOM (Saraph 1972, 1978). For elements with $Z \lesssim 26$ this procedure is much more economical than the full B-P treatment and yields collision strengths of comparable accuracy, except near threshold.

In its simplest form the transformation is purely algebraic:

$$X^{J\pi}(S_1L_1J_1l_1k_1, S_2L_2J_2l_2k_2) = \sum_{SL} X^{SL\pi}(S_1L_1l_1s_1, S_2L_2l_2s_2) \, C(SLJ, S_1L_1J_1, l_1k_1) C(SLJ, S_2L_2J_2, l_2k_2), \tag{20}$$

with the usual notation for the target and electron quantum numbers, and $\boldsymbol{k}_i = \boldsymbol{J}_i + \boldsymbol{l}_i$ such that $\boldsymbol{J} = \boldsymbol{k}_i + \boldsymbol{s}_i$. X stands for the K-matrix, the transmission matrix or the scattering matrix (Eq. 16) and

$$C\ (SLJ, S_iL_iJ_i, lk) = \sqrt{(2S+1)(2L+1)(2k+1)(2J_i+1)} \times\ W(LlS_iJ_i; L_ik) W(LJS_is; Sk) \tag{21}$$

where the functions W are Racah coefficients.

An optional extension of Eq. (20) accounts for effects of J-J coupling between the target terms. These can be included to first order by a second transformation,

$$X^{J\pi}(\Delta_1 J_1 k_1, \Delta_2 J_2 k_2) = \sum_{S_1L_1S_2L_2} X^{J\pi}(S_1L_1J_1k_1, S_2L_2J_2k_2) \, f_{J_1}(S_1L_1, \Delta_1) f_{J_2}(S_2L_2, \Delta_2). \tag{22}$$

The quantities f are term-coupling coefficients (TCCs). They can be obtained from the eigenvectors of the target Hamiltonians in LS coupling *and* intermediate coupling (cf. Jones 1975), and are calculated in either the atomic structure programs (Subsect. 2.1), or the R-matrix programs – an IRON Project development.

The new intermediate coupling collision programs for processing LS coupled matrices renormalize the TCCs so as to conserve flux. This makes possible a consistent treatment as the collision energy passes through the excitation threshold of each target term. Renormalisation is called for even when all channels are open, because of high lying correlation components of a CI type target — a point mostly overlooked previously, although the consequences were not serious, as the errors typically lay well below the 1% mark.

One can go one step further at practically no extra expense by carrying out the scattering calculation in *LS* coupling including mass correction and Darwin contributions; thus part of the relativistic corrections to the energies of the target and the (N+1) electron states are included, which would not have been achieved by the recoupling transformations alone; these are, of course, still required to complete the calculation (cf. Saraph & Storey 1993).

3. Theory of radiative transitions

The oscillator strength or photoionization cross section is proportional to the generalized line strength (Seaton 1987b) defined, in either length form or velocity form, by the equations

$$S_{\rm L} = \left| \left\langle \Psi_f | \sum_{j=1}^{N+1} z_j | \Psi_i \right\rangle \right|^2 \tag{23}$$

and

$$S_{\rm V} = \omega^{-2} \left| \left\langle \Psi_f | \sum_{j=1}^{N+1} \frac{\partial}{\partial z_j} | \Psi_i \right\rangle \right|^2 . \tag{24}$$

In these equations ω is the incident photon energy in Rydberg units, and Ψ_i and Ψ_f are the wave functions representing the initial and final states respectively. The boundary conditions satisfied by a bound state correspond to decaying waves in all channels, whilst those satisfied by a free state correspond to a plane wave in the direction of the ejected electron momentum $\hat{k}$ and ingoing waves in all open channels.

Both Ψ_i and Ψ_f are now expanded in terms of the R-matrix basis in the internal region defined by Eqs. (7) and (8). The

coefficients A_{ki} and A_{kf} in Eq. (8) are determined by solving the differential Eqs. (12) in the external region, subject to the boundary conditions discussed above, and matching to the R-matrix boundary condition at $r = a$. In the case of the initial bound states an iterative procedure for the energy has to be adopted to achieve this matching which involves the use of a special technique to carry out the calculation in the vicinity of R-matrix poles (Burke & Seaton 1984; Seaton 1985).

The non-relativistic R-matrix computer program of Berrington et al. (1974, 1978) has been considerably extended by Seaton (1987b) and Berrington et al. (1987) to enable the calculation of atomic bound-bound and bound-free photoabsorption data for the large number of ground and excited state atoms and ions required in the Opacity Project. The formulation was restricted to E1 transitions in LS coupling. The external-region modules for electron collisions, bound states, bound-bound data and photoionization in the LS coupling scheme (STGF, STGB, STGBB, and STGBF, respectively, as described by Berrington et al. 1987), have, for the IRON Project, been modified to accept data also in the intermediate coupling scheme.

3.1. Inclusion of E2 and M1 transitions in the R-matrix program

These programs now include the formalism required to calculate radiative data for E1 transitions, in both LS and intermediate coupling, and the accuracy obtained is generally good. Work is in progress enabling the BP version of the R-matrix package to calculate radiative quantities associated with electric quadrupole (E2) and magnetic dipole (M1) transitions as well. This involves some theoretical development as well as programming effort.

Appendix A gives details of the R-matrix method for the E2 case in the length formulation, which requires a fairly straightforward generalization of E1. Also in this first stage of development an elaborate programming effort will provide for M1 transitions, employing a radiative operator correct to full low-Z BP order, as implemented in SUPERSTRUCTURE (Eissner & Zeippen 1981). A second stage will deal with deficiencies of the radiative electric multipole operators in the velocity form, adding corrections of BP order. So far one serious gap remains in our programs, affecting near-neutral ions just highly enough ionized for fine structure to matter: namely the missing two-body fine structure terms of the BP Hamiltonian. Their absence is noticeable in particular for terms associated with half-filled shells, since ordinary spin-orbit effects vanish — it is only well above z=30 that second order ordinary spin-orbit coupling begins to dominate. Bridging this gap involves major developments.

4. The effective collision strength

In astrophysical and plasma applications it is often the excitation *rate coefficient* (q_{if}) which is needed, and in this context it is convenient to define the dimensionless thermally-averaged *effective collision strength* (Υ_{if}) as

$$\Upsilon_{if}(T) = \int_0^\infty \Omega_{if}(E_f) \mathrm{e}^{-E_f/kT} \mathrm{d}(E_f/kT) \qquad (25)$$

where E_f is the kinetic energy of the outgoing electron, T the electron temperature in K, and $k = 6.339 \times 10^{-6}$ Ryd/K is Boltzmann's constant. The excitation rate coefficient is then

$$q_{if} = \frac{8.63 \times 10^{-6} \mathrm{K}^{1/2}}{w_i T^{1/2}} \Upsilon_{if}(T) \mathrm{e}^{-\Delta E/kT} \ \mathrm{cm}^3\mathrm{s}^{-1}, \qquad (26)$$

and the de-excitation rate coefficient is

$$q_{fi} = \frac{8.63 \times 10^{-6} \mathrm{K}^{1/2}}{w_f T^{1/2}} \Upsilon_{if}(T) \ \mathrm{cm}^3\mathrm{s}^{-1}, \qquad (27)$$

where w_i and w_f are the statistical weights of the lower and upper states respectively, whose energy difference is ΔE. The collision stength is symmetric as well as dimensionless, i. e. $\Omega_{if} = \Omega_{fi}$ and $\Upsilon_{if} = \Upsilon_{fi}$.

4.1. Calculation of excitation rates and presentation of results

Although the integral in Eq. (25) is simple in form, it has to be evaluated numerically. To do this accurately can be difficult, for three reasons.

Firstly, the fact that Ω is calculated for energies up to some finite maximum value, which depends on the approximations made in the calculation, restricts the maximum temperature for which $\Upsilon(T)$ can be calculated without degrading the accuracy inherent in Ω.

Secondly, the complex resonance structures in Ω require the collision strength to be evaluated on a sufficiently fine energy grid.

Thirdly, the evaluation of the rate coefficient at very low temperatures is also difficult in many transitions because the location of resonances occurring just below and directly above the threshold must be accurately known; experimental values of the resonance energies are often not available.

The first two points are discussed further below; the third point will be returned to in subsection 5.1.

4.1.1. Availability of $\Omega(E)$ only for finite energies

Ω is normally calculated up to a finite maximum value of the energy, say $E_{\max}$, whereas the upper limit of the integation in Eq. (25) is infinite. There are two basic points of view in addressing this problem. One is to restrict the evaluation of rate coefficients to a specified finite temperature interval, determined by $E_{\max}$, such that the accuracy of $\Upsilon(T)$ is not affected by this limitation. The other is to extrapolate Ω to higher energies so as not to restrict the temperature range of $\Upsilon(T)$.

This latter method is adopted by Burgess & Tully (1992), in which the collision strength and energy are both suitably scaled and then plotted so that the behaviour of Ω at all energies can be visualized on a computer screen by means of a program called OMEUPS. Knowing the high energy Born limit value of the collision strength allows one to span the range between $E_{\max}$ and infinity with some confidence. A cubic spline curve is used for this purpose. The resulting values of Ω may be added to those of the R-matrix calculation and in this way the integral (25) is

calculated over the entire energy range. Details of how this may be done numerically are given in Burgess & Tully (1992).

In its present form OMEUPS requires human interaction, which makes it more appropriate for examining a few selected transitions. The approach also has a disadvantage that collision strengths for dipole forbidden transitions beyond $E_{\max}$ are inherently less accurate.

In subsequent papers of this series, numerical integration, possibly using OMEUPS, will be used but $\Upsilon(T)$ will be tabulated only for temperatures corresponding to the energy interval on which Ω is calculated.

4.1.2. Choice of energy mesh

If the electron energy E_f lies below an excited state threshold ϵ_i of a ionic target with residual charge z, it is convenient to introduce an effective quantum number ν such that

$$\epsilon_i - E_f = \frac{z^2}{\nu^2}. \tag{28}$$

Since a similar pattern of resonances occurs each time ν increases by unity, it is best to scan the resonances using a constant step-length $\Delta\nu$, rather than a constant ΔE_f.

In order to illustrate the errors that occur from insufficient energy resolution and to estimate the size of the increment in energy or effective quantum number necessary for accurate integration over a typical resonance structure, let us generate "synthetic" resonances from an analytic formula which simulates a realistic Ω. The corresponding $\Upsilon(T)$ can then be generated with arbitrarily high accuracy, providing a standard against which the errors arising from any integration mesh can be easily found.

Needless to say, this procedure is completely artificial and is not employed in our calculations of $\Upsilon(T)$, as complex multichannel resonance structures, which can overlap and interfere with each other, can not in general be reduced to simple analytic formulae.

The following formula simulates the effect of an open and a closed scattering channel with eight Rydberg series of isolated resonances converging to the higher state:

$$\Omega = \sum_{j=1,8} \frac{(1+\tau_j)(x_j+q_j)^2\,(b_j - c_j\nu^{-2})}{(1+\tau_j q_j^2)(1+x_j^2)(z+2)^2} + \Omega_{\rm b}. \tag{29}$$

$\Omega_{\rm b}$ is a constant background contribution with the value $15.5/(z+2)^2$, where z is the ion charge number. The notation used in Eq. (29) follows that of Dubau & Seaton (1984), namely

$$x_j = \tan[\pi(\nu+\alpha_j)]/\tau_j, \quad \tau_j = \tanh(\pi\beta_j). \tag{30}$$

The constants α_j, β_j, q_j, b_j and c_j were chosen to provide a rough fit to the resonances obtained in a two state R-matrix calculation for excitation of Fe XVIII with observed term energy splitting (to be discussed in detail in Subsect. 5.1). A graphical comparison is given in Fig. 1 for those resonances corresponding to the capture of an electron into states with $n = 6$. The resonances in Fig. 1(a) were calculated using the programs

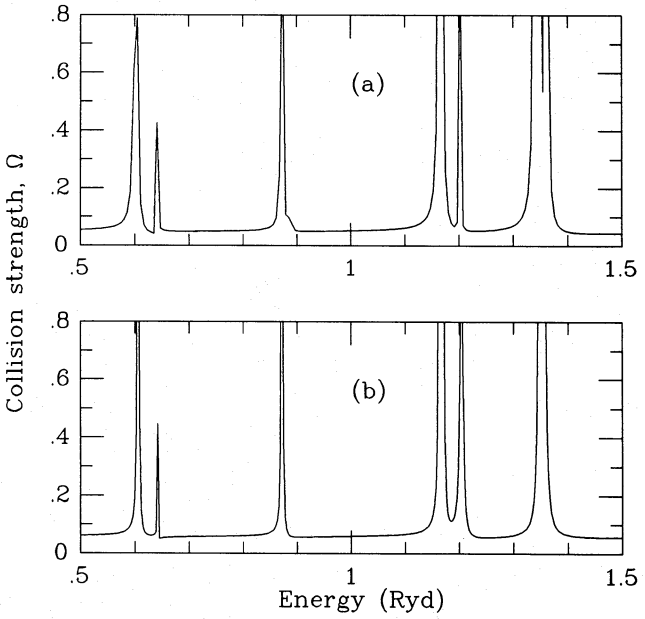

Fig. 1. a and b. Comparison of resonances caused by the capture of an electron into states with $n = 6$ in a two term calculation for Fe XVIII: **a** from an LS coupling R-matrix calculation with algebraic recoupling; **b** with synthetic resonances using Eq. (29)

RMATRX and JAJOM and Fig. 1(b) shows the synthetic resonances. A similar comparison over a much wider energy range is given in Figs. 2(a) and 2(b).

The resonances are calculated in the energy range $0.0 \le E_j/\text{Ryd} \le 6.21933$, corresponding to $5.547888 \le \nu \le 9.547888$. The Gailitis average is used in the interval from 6.21933 Ryd to the ^{2}S threshold at 9.3895 Ryd, with radiative damping effects included (cf. Seaton 1983). At higher energies the two-state collision strength is a slowly varying function of energy which tends towards the Born limit 0.0187 (see Tully 1986). The integral in Eq. (25) is evaluated by linearly interpolating Ω between adjacent energy points and integrating analytically over each interval in E_f/kT.

The results obtained for $\Upsilon(T)$ with different values for N (i.e. the total number of steps used to delineate the resonances having $n = 6, 7, 8, 9$) are compared in Table 1. This example shows that even with a steplength as small as $\Delta\nu = 0.01$ (i.e. $N = 400$), errors of the order of 25 per cent occur. It may be necessary to use an even smaller value than this in regions where Ω varies greatly and especially when resonances are narrow.

5. Detailed discussion of Fe XVIII

In order to illustrate recent developments of the IRON Project, consider the scattering of electrons from F-like Fe XVIII.

The next two subsections are concerned with fine structure transitions in electron scattering from Fe XVIII, and bound-bound and bound-free transitions in Fe XVII. In each case, a fluorine-like target of nine electrons is considered. For radiative calculations, the neon-like states are represented by a colli-

Table 1. $100 \times \Upsilon(T)$ calculated using a synthetic collision strength consisting of the parametric expression (29) to delineate the resonances in the range from $E_f = 0$ to $E_f = 6.21933$ and the 2-state close-coupling approximation for energies beyond 6.21933 Ryd. N is the number of equidistant steps used to span the interval from $\nu = 5.547888$ to $\nu = 9.547888$. The steplength $\Delta\nu = 4/N$

log T	N = 4000	N = 3000	N = 2000	N = 1000	N = 800	N = 600	N = 400
+4.0	5.783	5.784	5.784	5.785	5.783	5.783	5.783
+4.5	6.213	6.245	6.301	6.586	6.114	6.232	6.288
+5.0	8.389	8.490	8.565	9.063	8.360	8.822	9.833
+5.5	9.110	9.201	9.236	9.385	9.343	9.808	11.390
+6.0	7.773	7.827	7.841	7.868	7.959	8.255	9.291
+6.5	5.528	5.549	5.555	5.559	5.609	5.734	6.169
+7.0	3.757	3.764	3.766	3.767	3.785	3.829	3.980
+7.5	2.589	2.591	2.592	2.592	2.598	2.612	2.662
+8.0	2.012	2.013	2.013	2.013	2.015	2.020	2.036

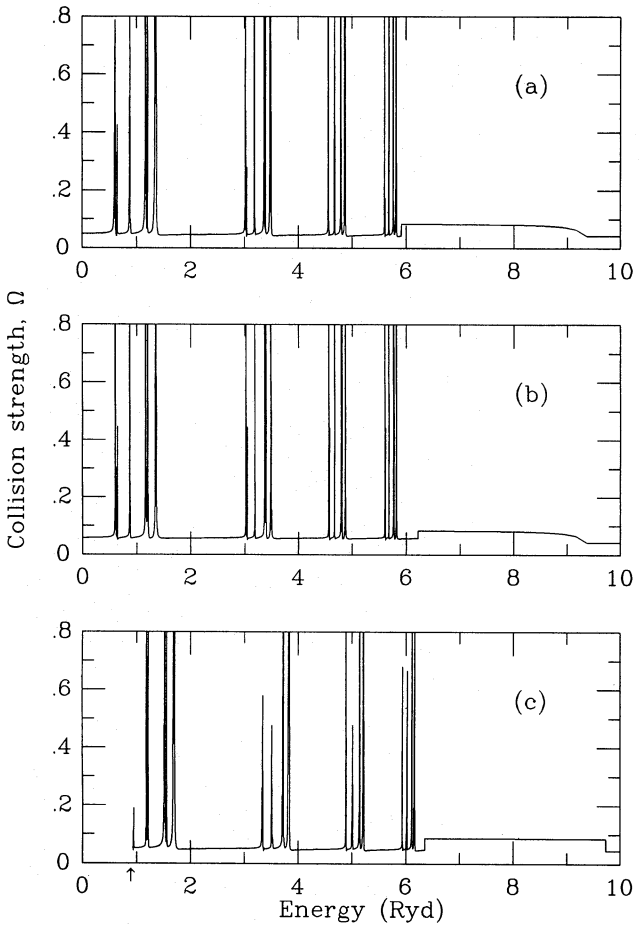

Fig. 2. a–c. Comparison of resonances converging to the ^{2}S threshold in a two term calculation for Fe XVIII: **a** from an LS coupling R-matrix calculation with algebraic recoupling; **b** with synthetic resonances using Eq. (29); **c** from a BP R-matrix calculation. The arrow on the energy axis indicates the threshold for the fine structure transition

sional R-matrix wavefunction of the electron plus fluorine-like target, so the procedures are similar to electron scattering from Fe XVIII.

There are two (n=2) ground complex terms in the target: $(1s^2 2s^2 2p^5)\,^2P^o$ and $(1s^2 2s 2p^6)\,^2S$, which split into three fine structure levels of $(J)^\pi = (3/2)^o$, $(1/2)^o$ and $(1/2)^e$. Including the configurations $(1s^2 2s^2 2p^4)3l$, where l = s, p, or d, gives 28 terms or 60 levels. Including all the so-called n = 3 terms, i.e. the above, together with $(1s^2 2s 2p^5)3l$ and $(1s^2 2p^6)3l$, totals 52 terms or 112 levels. This shows that the scale of the calculation can change dramatically if a complete set of configurations with one n = 3 electron is to be included, particularly for fine structure transitions.

Previous calculations have been carried out in the 2-term and 28-term approximations in LS coupling. Two target orbital sets have been used. In the 2-term Opacity Project calculation of Hibbert & Scott (1993), the orbitals are 1s, 2s, 2p, $\overline{3}$d, with the $\overline{3}$d being a correlation orbital optimized on the $(1s^2 2s^2 2p^5)\,^2P^o - (1s^2 2s 2p^6)\,^2S$ oscillator strength. In the 28-term electron scattering calculation of Mohan et al. (1987a,b), the 1s, 2s, 2p, 3s, 3p, 3d orbitals are all spectroscopic.

The next two subsections examine the different approximations and inclusion of relativisic effects.

5.1. Electron impact excitation of fine structure transitions in Fe XVIII

The fine structure transition within the ground term $(1s^2 2s^2 2p^5)\,^2P^o_{3/2} - ^2P^o_{1/2}$ is discussed here.

The effective collision strength evaluated in the two-term approximation (cf. Subsect. 4.1.2) in LS coupling with algebraic recoupling, is shown in Fig. 3. The resonances in Ω which converge to the ^{2}S threshold produce a noticeable bump in $\Upsilon(T)$ centred near 3×10^5 degrees Kelvin.

However, the fine structure splitting of the $^2P^o$ ground state, 0.9354 Ryd affects the shape of $\Upsilon(T)$ at the lower temperatures. Scattering data obtained from a calculation in LS coupling differ from those obtained in a full BP treatment, in that the latter obtain non-zero energies for the fine structure splitting

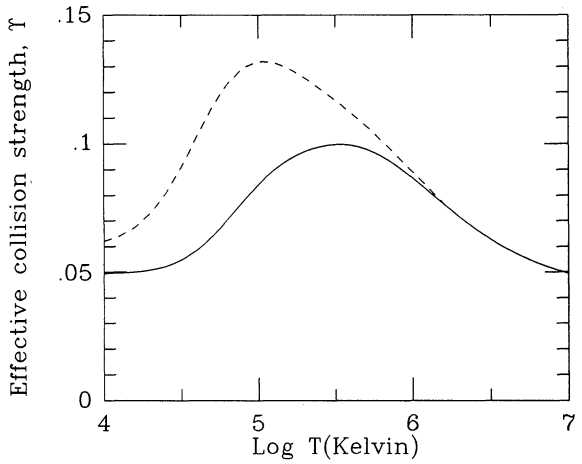

Fig. 3. Comparison of $\Upsilon(T)$ for $(^2P^o_{3/2}-^2P^o_{1/2})$ in Fe XVIII: —, from a 2-term LS coupling R-matrix calculation with algebraic recoupling; - - -, from a 3-level BP R-matrix calculation

of the levels, and slightly different effective quantum numbers for the Rydberg series. When calculating collision rates, the first discrepancy can be compensated for by shifting the energy scale. The second discrepancy can have large effects on $\Upsilon(T)$ at low temperatures if there are resonances close to the excitation threshold. A BP R-matrix calculation of the resonance structure, using the same two-term model and orbitals, is shown in Fig. 2c. The resulting $\Upsilon(T)$, plotted for comparison in Fig. 3, shows deviations from the recoupling approach at low temperatures. The BP R-matrix approach is the best one in such circumstances.

It should be noted that Mohan et al. (1987a and 1987b), who used a 28-term R-matrix calculation with algebraic recoupling, obtained an $\Upsilon(T)$ 'bump' for this transition extending to higher temperatures, due to resonances associated with the n=3 terms. This work will be repeated in the IRON Project because the energy mesh used has been found to be inadequate for an accurate calculation of collision rates.

5.2. Radiative data for fine structure transitions in Fe XVII

Presented here are some calculations using the new IRON Project developments to calculate radiative data for electric dipole (E1) transitions between fine structure levels.

The 28-term, 60 level, F-like Fe target is used here, together with the new BP R-matrix program. Table 2 compares the gf-values obtained for a few fine structure levels in Fe XVII with those from other theoretical calculations. A major advantage of the R-matrix method is that highly excited bound states can be treated with an accuracy similar to that for the lower bound states.

Fig. 4 shows the cross section for photoionizing the lowest two $J = 0^e$ fine structure levels in Fe XVII. The photon energy range displayed is in the interval between the $(1s^22s^22p^5)^2P^o_{3/2}$ and $^2P^o_{1/2}$ ionization thresholds. Previous calculations (e.g. for the Opacity Project, Hibbert & Scott 1993) have been in LS coupling, with the two levels assumed degenerate. This is therefore

Table 2. gf-values for transitions involving the lowest two $J = 0^e$ levels in Fe XVII, using the BP R-matrix method with a 60 level F-like target. The $J = 1^o$ levels are examined up to $n_{\rm eff}$=4.9, where $17^2/n^2_{\rm eff}$ Ryd is the calculated ionization energy relative to the $(2p^5)^2P_{3/2}$ ground level of Fe XVIII (the two $J = 0^e$ levels have a calculated $n_{\rm eff}$ of 1.7645 and 2.8256 respectively). BFS and ZS are the gf-values calculated by Bhatia et al. (1985) and Zhang & Sampson (1989)

		$n_{\rm eff}$	gf	BFS	ZS
$(2p^6)^1S_0$	$-(2p^53s)^1P_1$	2.7115	0.122	0.111	0.112
	$-(2p^53s)^3P_1$	2.7423	0.103	0.106	0.096
	$-(2p^53d)^3P_1$	2.9260	0.0075	0.0073	0.010
	$-(2p^53d)^3D_1$	2.9596	0.610	0.522	0.600
	$-(2p^53d)^1P_1$	3.0053	2.34	2.61	2.48
	$-(2s2p^63p)^3P_1$	3.2697	0.0349		0.036
	$-(2s2p^63p)^1P_1$	3.2895	0.285		0.296
	$-(2p^54s)^1P_1$	3.7187	0.0231		0.019
	$-(2p^54s)^3P_1$	3.8081	0.0177		0.013
	$-(2p^54d)^3P_1$	3.9247	0.0031		0.004
	$-(2p^54d)^3D_1$	3.9593	0.368		0.385
	$-(2p^54d)^1P_1$	4.0611	0.394		0.441
	$-(2p^55s)^1P_1$	4.7201	0.0098		
	$-(2p^55s)^3P_1$	4.9060	0.0136		
$(2p^53p)^3P_0$	$-(2p^53s)^1P_1$	2.7115	0.102	0.097	
	$-(2p^53s)^3P_1$	2.7423	0.0285	0.0312	
	$-(2p^53d)^3P_1$	2.9260	0.0095	0.0108	
	$-(2p^53d)^3D_1$	2.9596	0.203	0.215	
	$-(2p^53d)^1P_1$	3.0053	0.0143	0.0143	
	$-(2s2p^63p)^3P_1$	3.2697	0.0318		
	$-(2s2p^63p)^1P_1$	3.2895	0.0229		
	$-(2p^54s)^1P_1$	3.7187	0.0059		
	$-(2p^54s)^3P_1$	3.8081	0.0667		
	$-(2p^54d)^3P_1$	3.9247	0.202		
	$-(2p^54d)^3D_1$	3.9593	0.141		
	$-(2p^54d)^1P_1$	4.0611	0.0095		
	$-(2p^55s)^1P_1$	4.7201	0.0012		
	$-(2p^55s)^3P_1$	4.9060	0.0099		

the first time that the photoionization cross section has been calculated at energies between the fine structure levels of the residual ion, and also the first time that photoionization cross sections have been calculated from excited states in intermediate coupling for a complex Fe ion.

6. Summary and outlook

The basic equations and the approximations employed in the IRON Project have been sketched, and the computer programs have been listed with references giving further information. Although development work and program checking continues, we are now in a position to generate accurate values for certain types of collisional and radiative rates of astrophysical interest.

The first stage of the Project is nearly complete, namely calculations of the fine structure collision rates in the ground

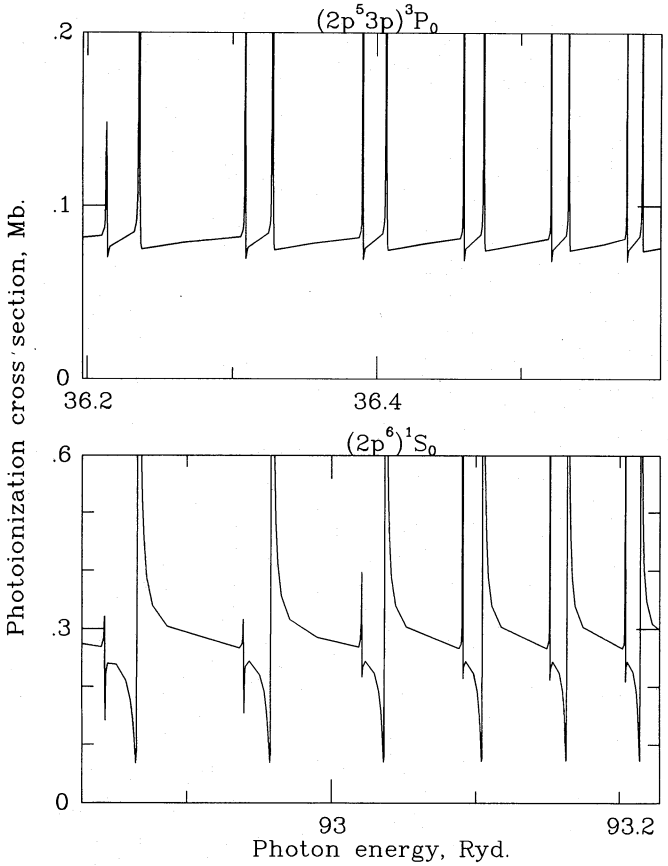

Fig. 4. Cross sections for photoionizing the two lowest $J = 0^e$ fine structure levels in Fe XVII, using the BP R-matrix method with a 60 level F-like target. The photon energy range begins at the $^2P^o_{3/2}$ ionization threshold (92.828 and 36.197 Ryds, for the two initial states shown), and shows resonances converging to the $^2P^o_{1/2}$ threshold

configuration for elements in the iso-electronic sequences B, C, O, F, Al, Si, S, and Cl. Results will be presented in further papers of the Series – Atomic Data from the IRON Project – in the A&A and A&AS.

The second stage, calculations for the ions of Fe as described in the Introduction, is underway; the first results should be available in 1994. Nearby elements will also be considered. We welcome inquiries and suggestions for further calculations.

Acknowledgements. We acknowledge the support and assistance of other members of the IRON project, including P.G. Burke, V.M. Burke, K. Butler A. Hibbert, M. Le Dourneuf, D.J. Lennon, H.E. Mason, C. Mendoza, M.P. Scott, M.J. Seaton, P.J. Storey, K.T. Taylor, C.J. Zeippen. We also thank M.J. Barlow for bringing to our attention the need for collisional rates for fine structure transitions in the analysis of ISO spectra with a detailed discussion of which lines are likely to be important. The UK participation in the IRON project is supported by the Science and Engineering Research Council grant GR/H93576. AKP acknowledges partial support from the U.S. National Science Foundation (PHY-9115057). We thank K. Butler and D.J. Lennon for assistance in preparing the manuscript.

Appendix A: E2 transitions in the R-matrix method

Given here, for the first time, are details of the R-matrix method for the E2 case in the length formulation, which is a fairly straightforward generalization of E1. This concerns in particular the calculation of the internal region reduced matrix elements in Eqs. (23) and (24) of the form $\langle\psi_k\|M^{[\kappa]}\|\psi_{k'}\rangle$, where $M^{[\kappa]}$ represents the electric moment operator corresponding to an E1 or E2 transition (κ = 1 or 2 respectively). Due to the fact that the total angular momentum and parity are not conserved in the initial and final states there are four types of matrix element arising from the use of the R-matrix basis Eq. (7): (i) continuum-continuum, (ii) bound-continuum, (iii) continuum-bound and (iv) bound-bound. These are first evaluated in LS coupling and then transformed as follows:

(i) continuum-continuum

$$\left\langle \Delta_i(J_i l_i)K_i\frac{1}{2}; J\pi\|M^{[\kappa]}\|\Delta_j(J_j l_j)K_j\frac{1}{2}; J'\pi'\right\rangle =$$

$$\sum_{LL'SC_iL_iS_iC_jL_jS_j}\sqrt{(2J+1)(2J'+1)}(-1)^{L'+S-J-\kappa}W(J'L'JL;S\kappa)$$

$$\times C(\Delta_i J_i; C_iL_iS_il_iK_i\frac{1}{2}LS; J\pi)C(\Delta_j J_j; C_jL_jS_jl_jK_j\frac{1}{2}L'S; J'$$

$$\times\left\langle C_i(L_il_i)L(S_i\frac{1}{2})S\pi\|M^{[\kappa]}\|C_j(L_jl_j)L'(S_j\frac{1}{2})S\pi'\right\rangle; \quad (31)$$

(ii) bound-continuum

$$\left\langle LS; J\pi\|M^{[\kappa]}\|\Delta_i(J_il_i)K_i\frac{1}{2}; J'\pi'\right\rangle =$$

$$\sum_{L'C_iL_iS_i}\sqrt{(2J+1)(2J'+1)}(-1)^{L'+S-J-\kappa}$$

$$\times W(J'L'JL;S\kappa)C(\Delta_iJ_i;C_iL_iS_il_iK_i\frac{1}{2}L'S;J'\pi')$$

$$\times\left\langle LS\pi\|M^{[\kappa]}\|C_i(L_il_i)L'(S_i\frac{1}{2})S\pi'\right\rangle; \quad (32)$$

(iii) continuum-bound

$$\left\langle \Delta_i(J_il_i)K_i\frac{1}{2}; J\pi\|M^{[\kappa]}\|L'S; J'\pi'\right\rangle =$$

$$\sum_{LC_iL_iS_i}\sqrt{(2J+1)(2J'+1)}(-1)^{L'+S-J-\kappa}$$

$$\times W(J'L'JL;S\kappa)C(\Delta_iJ_i;C_iL_iS_il_iK_i\frac{1}{2}LS;J\pi)$$

$$\times\left\langle C_i(L_il_i)L(S_i\frac{1}{2})S\pi\|M^{[\kappa]}\|L'S\pi'\right\rangle; \quad (33)$$

(iv) bound-bound

$$\left\langle LS; J\pi\|M^{[\kappa]}\|L'S; J'\pi'\right\rangle =$$

$$\sqrt{(2J+1)(2J'+1)}(-1)^{L'+S-J-\kappa}W(J'L'JL;S'\kappa)$$

$$\times\left\langle LS\pi\|M^{[\kappa]}\|L'S\pi'\right\rangle; \quad (34)$$

where the notation is as described in subsection 2.6. At this stage, the velocity operators for electric multipole radiation will be left in their non-relativistic form.

References

Baluja K.L., Burke P.G. and Morgan L.A., 1982, Comput. Phys. Commun. 27, 299

Berrington K.A., Burke P.G., Chang J.J., Chivers A.T., Robb W.D. and Taylor K.T., 1974, Comput. Phys. Commun. 8, 149

Berrington K.A., Burke P.G., Le Dourneuf M., Robb W.D., Taylor K.T. and Vo Ky Lan, 1978, Comput. Phys. Commun. 14, 367

Berrington K.A., Burke P.G., Butler K., Seaton M.J., Storey P.J., Taylor K.T. and Yu Yan, 1987, J. Phys. B: Atom. Mol. Phys. 20, 6379

Bhatia A.K., Feldman U. and Seely J.F., 1985, Atom. Data Nucl. Data Tables 32, 435

Blume M. and Watson R.E. 1962, Proc. R. Soc. 270A, 127

Burgess A. and Tully J.A., 1992, A&A, 254, 436

Burke P.G., Hibbert A. and Robb W.D., 1971, J. Phys. B: Atom. Mol. Phys. 4, 153

Burke P.G., Berrington K.A., and Sukumar C.V., 1981, J. Phys. B: Atom. Mol. Phys. 14, 289

Burke P.G. and Eissner W., 1983, in: Atoms and Astrophysics, eds. P.G. Burke, W.Eissner, D.G. Hummer and I.C. Percival, Plenum, New York, p. 1

Burke P.G. and Seaton M.J., 1984, J. Phys. B: Atom. Mol. Phys. 17, L683

Burke P.G., Noble C.J.. and Scott M.P., 1987, Proc. R. Soc. A 410, 289

Burke V.M. and Seaton M.J., 1986, J. Phys. B: Atom. Mol. Phys. 19, L527

Buttle P.J.A., 1967, Phys. Rev. 160, 719

Clementi E. and Roetti R., 1974, At. Data Nucl. Data Tables 14, 177

Cunto W. and Mendoza, C., 1992, Rev. Mex. Astron. Astrofis. 23, 107

Dubau J. and Seaton M.J., 1984, J. Phys. B: Atom. Mol. Phys. 17, 381

Eissner W., 1991, J. Physique IV (Paris) C1, 3

Eissner W., Jones M. and Nussbaumer H., 1974, Comput. Phys. Commun. 8, 270

Eissner W. and Zeippen C.J., 1981, J. Phys. B: Atom. Mol. Phys. 14, 2125

Henry R.J.W., 1993, Rept. Prog. Phys. 56, 327

Hibbert A., 1975, Comput. Phys. Commun. 9, 141

Hibbert A. and Scott M.P., 1993, J. Phys. B: Atom. Mol. Phys. , in press

Jones M., 1975, Phil. Trans. Roy. Soc. London 277, 588

Le Dourneuf M., Vo Ky Lan and Zeippen C.J., 1979, J. Phys. B: Atom. Mol. Phys. 12, 2449

Light J.C. and Walker R.B., 1976, J. Chem. Phys. 65, 4272

Light J.C., Walker R.B., Stachel E.B. and Schmalz T.G., 1979, Comput. Phys. Commun. 17, 89

Mohan M., Baluja K.L., Hibbert A. and Berrington K.A., 1987, Mon. Not. R. astr. Soc. 225:2, 377

Mohan M., Baluja K.L., Hibbert A. and Berrington K.A., 1987, J. Phys. B: Atom. Mol. Phys. 20, 6319

Noble C.J. and Nesbet R.K., 1984, Comput. Phys. Commun. 33, 399

Noble C.J. and Burke V.M., 1993, Comput. Phys. Commun. , in press

Norrington P.H. and Grant I.P., 1981, J. Phys. B: Atom. Mol. Phys. 14, L261

Norrington P.H. and Grant I.P., 1987, J. Phys. B: Atom. Mol. Phys. 20, 4869

Nussbaumer H. and Storey P.J., 1978, A&A 64, 139

Saraph H.E., 1972, Comput. Phys. Commun. 3, 256

Saraph H.E., 1978, Comput. Phys. Commun. 15,247

Saraph H.E. and Storey P.J., 1993, to be submitted

Scholz T.T., Walters H.R.J., Burke P.G., and Scott M.P., 1990, Mon. Not. R. astr. Soc. 242, 692

Scott N.S. and Burke P.G., 1980, J. Phys. B: Atom. Mol. Phys. 13, 4299

Scott N.S. and Taylor K.T., 1982, Comput. Phys. Commun. 25, 349

Seaton M.J., 1983, Reports on Progress in Physics 46, 167

Seaton M.J., 1985, J. Phys. B: Atom. Mol. Phys. 18, 2111

Seaton M.J., 1987a, J. Phys. B: Atom. Mol. Phys. 20, L69

Seaton M.J., 1987b, J. Phys. B: Atom. Mol. Phys. 20, 6363

Seaton M.J., Yu Y., Mihalas D. and Pradhan A.K., 1993, MNRAS, in press

Tully J.A., 1986, 11ème Colloque sur la Physique des Collisions Atomiques et Electroniques, Metz 18–20 juin

Viotti R., Vittone A., and Friedjung M., eds., 1988, IAU Colloquium 94, Physics of formation of Fe II lines outside LTE, Reidel, Dordrecht

Zhang H.L. and Sampson D.H., 1989, Atom. Data Nucl. Data Tables 43, 1

This article was processed by the author using Springer-Verlag LaTeX A&A style file version 3.